Frequency-octupled phase-coded signal generation based on carrier-suppressed high-order double sideband modulation

Xuan Li (李 轩)[1,2,*], Shanghong Zhao (赵尚弘)[1], Zihang Zhu (朱子行)[1], Kun Qu (屈 坤)[1], Tao Lin (林 涛)[1], and Shilong Pan (潘时龙)[2]

[1]*Information and Navigation College, Air Force Engineering University, Xi'an 710077, China*
[2]*Key Laboratory of Radar Imaging and Microwave Photonics, Ministry of Education, Nanjing University of Aeronautics and Astronautics, Nanjing, 210016, China*
**Corresponding author: lixuanrch@163.com*

Received January 10, 2017; accepted April 7, 2017; posted online April 24, 2017

An approach for photonic generation of a frequency-octupled phase-coded signal based on carrier-suppressed high-order double sideband modulation is proposed and experimentally demonstrated. The key component of the scheme is an integrated dual-polarization quadrature phase shift keying modulator, which is used to achieve the carrier-suppressed high-order double sideband modulation. At the output of the modulator, two fourth-order optical sidebands are generated with the optical carrier suppressed. After that, a Sagnac loop incorporating a fiber Bragg grating and a phase modulator is employed to separate the two optical sidebands and phase modulate one sideband with a binary coding signal. The approach features large carrier frequency tuning range for the generated phase-coded signal from several megahertz to beyond the W-band. A proof-of-concept experiment is carried out. The 2 Gbit/s phase-coded signals with frequencies of 16.48, 21.92, and 29.76 GHz are generated.

OCIS codes: 060.2330, 060.5625, 120.5060.
doi: 10.3788/COL201715.070603.

The operation frequency of phase-coded signals applied in modern radar and communication systems is developing toward high frequency bands[1,2]. In this regards, the phase-coded signals cannot be easily accomplished by electronic techniques due to the limited speed and bandwidth of electronic devices. Thanks to the intrinsic advantages of high frequency, wide bandwidth, and large tunability, photonic techniques can provide capabilities of generating and processing a microwave or millimeter-wave signal with much higher frequency and better tunability[3–6].

One typical photonic method to generate a phase-coded signal is using optical spectral shaping combined with the wavelength-to-time mapping technique. The spectral shaper can be a spatial light modulator (SLM)[7], and it can provide good reconfigurability for the generated waveform, but the system is bulky and lossy due to the use of a free-space optical device. The spectral shaper can also be a specially designed fiber Bragg grating (FBG) with high integration and slight weight[8], but the system has poor tunability due to the fixed spectral response of the FBG. The second method to photonic generation of a phase-coded signal is by using the optical carrier phase-shifting technique, which is usually achieved by employing an integrated modulator[9,10]. In this method, one branch of the modulator is modulated with a radio frequency (RF) signal to generate carrier-suppressed optical sidebands, while another branch is modulated with a coding signal to change the phase of the optical carrier. However, the carrier frequency of the generated phase-coded signal is limited by the operation bandwidth of the modulator. The third method to generate a phase-coded signal is by introducing a phase difference between two optical wavelengths[11–15]. In this method, two optical sidebands are first generated, then, a phase modulator (PM) or a polarization modulator (PolM) is utilized to achieve the phase coding operation. The frequency multiplication can be achieved by using this method to improve the frequency bound of the phase-coded signal. For example, frequency-doubled and -quadrupled phase-coded signals have been generated[12–15]. However, the frequency-doubled signal can hardly support high frequency applications, while the frequency-quadrupled signal has limited tunability due to the use of a polarization-maintaining FBG. To achieve high frequency phase-coded signal generation, the method based on beating two optical sidebands of a modulated phase-coded signal can be utilized, in which an electrical phase-coded signal is first generated and then modulated to the optical domain; after that, an optical filter (OF) is followed to select two high-order optical sidebands[16,17]. A frequency-octupled phase-coded signal has been generated by using this method, however, the phase coding is implemented in the electrical domain, and the OF limits the frequency tunability.

Previously, we have proposed a scheme to generate a phase-coded signal by using a quadrature phase shift keying (QPSK) modulator, a Sagnac loop, and a PolM[18]. The carrier frequency of the generated phase-coded signal is four times the frequency of the driving RF signal, making the system have a large frequency tuning range. In this Letter, the works have been developed around the further

 © 2017 Chinese Optics Letters

improvement of the operation frequency and tunability. Thanks to the use of an integrated dual-polarization QPSK (DP-QPSK) modulator, the frequency-octupled operation is achieved. A phase-coded signal with the central frequency ranged from several megahertz (MHz) to beyond the W-band can possibly be generated. To the best of our knowledge, it is the largest frequency tuning range ever achieved for a photonic generated phase-coded signal.

Figure 1 shows the principle diagram of the proposed frequency-octupled phase-coded signal generation system. A tunable laser source (TLS) is used to generate a light with its polarization adjusted by a polarization controller (PC). The light is sent to a DP-QPSK modulator, which is an integrated device including a 3 dB optical coupler (OC), two parallel QPSK modulators, and a polarization beam combiner (PBC). A microwave signal generator (MSG) is employed to provide an RF signal. The RF signal is then divided into two paths and applied to the two RF ports of the upper QPSK modulator. An electrical phase shifter is inserted in one path to generate a phase difference of $\pi/2$. The bottom QPSK modulator is only direct current (DC) biased. All of the sub-Mach–Zehnder modulators (MZMs) and main MZMs of the two QPSK modulators are biased at the maximum transmission point. The optical signals from two QPSK modulators are combined and orthogonally polarized through the PBC. The output optical signal of the DP-QPSK modulator is

$$\vec{E}_m(t) \propto \sum_{n=-\infty}^{\infty} \vec{x}\, J_{4n}(m)\exp(j\omega_c t + 4n\omega t) + \vec{y}\exp(j\omega_c t), \tag{1}$$

where ω is the angular frequency of the RF signal, m is the modulation index, J_n is the nth-order Bessel function of the first kind, x and y directions represent the two orthogonal principal axes of the PBC. As can be seen, the output signal of the modulator has two parts aligned along two orthogonal polarization directions, respectively.

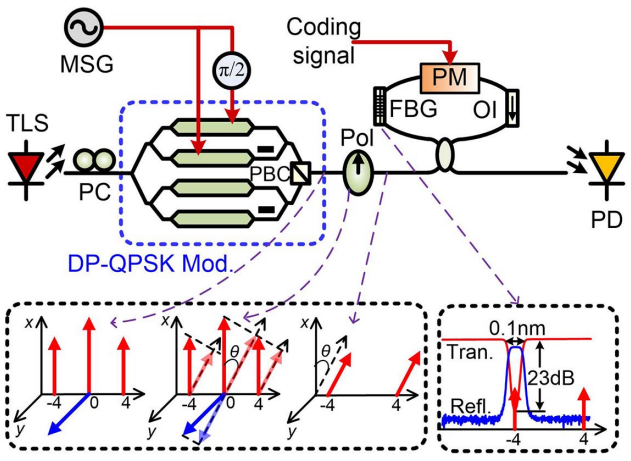

Fig. 1. Proposed frequency-octupled phase-coded signal generation system.

In one direction, the optical signal has carrier and two fourth-order sidebands, while in another direction, the optical signal has only the carrier component.

After the PBC, a polarizer (Pol) is utilized with its principal axis having an angle of ϑ relative to the x direction. When the high-order sidebands are neglected, the output signal of the Pol is

$$E_{pol}(t) \propto [J_0(m)\cos\theta + \sin\theta]\exp(j\omega_c t) + J_4(m)\cos\theta\exp(j\omega_c t \pm 4\omega t). \tag{2}$$

Therefore, two fourth-order sidebands can be obtained with the optical carrier suppressed by satisfying $J_0(m)\cos\theta + \sin\theta = 0$. As a result, the carrier-suppressed high-order double sideband modulation is achieved by using a single modulator, as shown in the inset of Fig. 1.

After that, the generated two fourth-order sidebands are put into a Sagnac loop. In the loop, an optical isolator (OI) is inserted to block the counter-clockwise transmitted optical signal. While for the clockwise transmitted optical signal, the −4th-order sideband is reflected back by an incorporated FBG, and the +4th-order sideband is passed through, as shown in the inset of Fig. 1. Therefore, the two sidebands are separated. After that, the +4th-order sideband is modulated with an electrical coding signal through a PM. At the output of the loop, the optical signal is given by

$$E_{out}(t) \propto J_4(m)\exp(j\omega_c t)\{\exp(-4\omega t) + \exp[4\omega t + \beta s(t)]\}, \tag{3}$$

where β is the modulation index of the PM, and $s(t)$ is the normalized waveform of the coding signal.

After optical to electrical conversion through a photodetector (PD), a frequency-octupled phase-coded waveform is obtained as

$$i(t) \propto J_4^2(m)\cos[8\omega t + \beta s(t)]. \tag{4}$$

The proposed scheme has good frequency tunability. The key point of the frequency tuning operation in the scheme is that both of the frequencies of the RF signal and the TLS should be tuned to make the −4th-order optical sideband reflect back and the +4th-order optical sideband pass through the incorporated FBG in the Sagnac loop. To realize the automatic control of the laser source, an optical power monitor can be inserted to obtain the control information and feedback to adjust the frequency of the TLS, according to the frequency tuning of the RF signal, as demonstrated in Ref. [18].

For the generated frequency-octupled phase-coded signal, the minimum carrier frequency is limited by the notch bandwidth of the FBG, which can be as small as a few MHz[19]. On the other hand, the maximum carrier frequency is eight times the operation bandwidth of the modulator and the microwave devices. Therefore, a phase-coded signal with high frequency and large

tunability can be achieved, and the carrier frequency of the generated phase-coded signal can be ranged from several MHz to beyond the W-band.

A proof-of-concept experiment is demonstrated. In the experiment, a 0.1 nm bandwidth notched FBG with a central wavelength of 1551.090 nm and notch deep of 23 dB is used, as shown in Fig. 1. A 13 dBm light is generated from a TLS (Agilent N7714A) and then put into a DP-QPSK modulator (Fujitsu FTM7977HQA) to modulate with a 23 dBm RF signal, which is generated from an MSG (Agilent E8257D). The electrical coding signal is provided by a pulse pattern generator (Anritsu MP1763C), and then sent to a 40 GHz bandwidth PM (EOSPACE PM-DV5-40). The detection is performed by a 40 GHz bandwidth PD (u2t XPDV2120R). The optical and electrical spectra are measured by an optical spectrum analyzer (Yokogawa AQ6370C) and a digital storage oscilloscope (Agilent DSO-X 92504A), respectively.

Figure 2 shows the observed optical spectra when the laser source is set to 1551.174 nm and the MSG is tuned to 2.74 GHz. First, the RF signals are applied to the two RF ports of the upper QPSK modulator, respectively. By adjusting the three DC bias points of this modulator, optical carrier and fourth-order sidebands can be generated at the output of the DP-QPSK modulator. Then, another PC followed by a polarization beam splitter (PBS) is connected to the output of the DP-QPSK modulator temporarily to separate the two optical signals of the two QPSK modulators. By adjusting the PC, an optical carrier can be obtained after one port of the PBS, and it represents the output signal of the bottom QPSK modulator, while after another port of the PBS, the output signal from the upper QPSK modulator can be obtained. Figure 2(a) shows the output optical spectra of the DP-QPSK modulator, and the upper and the bottom QPSK modulators, respectively. It can be seen that, the two optical signals from the two QPSK modulators are separate well after the two ports of the PBS, which means that the two signals are orthogonally polarized. After that, the three DC bias points of the bottom QPSK modulator are set to the maximum transmission points. By adjusting the principal axis of the Pol, the two optical carrier components can be canceled by each other. Figure 2(b) shows the output optical spectrum of the Pol. It can be seen that, the carrier-suppressed high-order double sideband modulation is successfully achieved. Two fourth-order sidebands are obtained with the optical carrier efficiently suppressed, and the power of the fourth-order sidebands is 20 dB higher than that of the other residual sidebands.

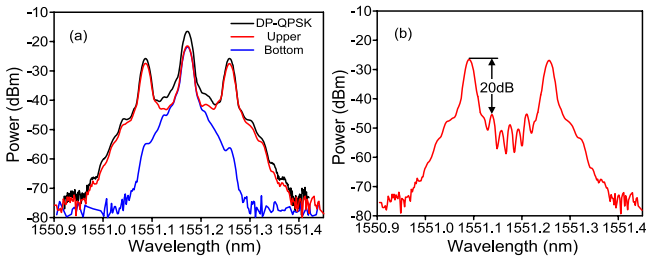

Fig. 2. Output optical spectra of (a) the integrated modulator, and the upper and bottom QPSK modulators and (b) the Pol.

In the Sagnac loop, one of the sidebands is phase modulated by a 2 Gbit/s binary coding signal with a fixed pattern of "1010." The output signal of the loop is boosted by an erbium-doped fiber amplifier (EDFA) and put into a PD. A DC blocker is used before the oscilloscope to remove the DC component. Figures 3(a) and 3(b) show the measured waveforms of the generated 21.92 GHz phase-coded signals with a time duration of 3 ns when the coding signal has a voltage of 1.5 and 2 V, respectively. The PM has a half-wave voltage of about 4 V, therefore, the theoretically calculated phase shifts of the waveforms in Figs. 3(a) and 3(b) are 135° and 180°, respectively. Figure 3(c) shows the extracted phase shifts from Figs. 3(a) and 3(b), which are consistent with the theoretical prediction.

To investigate the pulse compression capability, a 5 Gbit/s 128 bit pseudo-random bit sequence (PRBS) with an amplitude of 2 V is applied to the PM. The waveform of the generated signal and the corresponding extracted phase shift are shown in Figs. 4(a) and 4(b), respectively, with a time duration of 5 ns. Figure 4(c) shows the autocorrelation result of the generated waveform. The peak-to-sidelobe ratio (PSR) is about 7 dB. The full width at half-maximum (FWHM) of the peak pulse is about 0.21 ns, as shown in the inset of the figure, leading to a compression ratio of about 121.9 (25.6/0.21).

The frequency tunability is also investigated. A 2 Gbit/s binary coding signal with a fixed pattern of "1010" and an amplitude of 2 V is applied to the PM. The MSG is set to 2.06 GHz and the laser source is adjusted to 1551.160 nm. Figure 5(a) shows the generated 16.48 GHz phase-coded waveform with a time duration of 3 ns. In another study, the MSG is tuned to 3.72 GHz, and the laser source is adjusted to 1551.212 nm. Figure 5(b) shows the generated 29.76 GHz phase-coded waveform with a time duration of 3 ns. Figure 5(c) shows the corresponding extracted phase shift from Figs. 5(a) and 5(b), respectively. Thanks to the frequency-octupled operation, the carrier frequency of the generated phased-coded

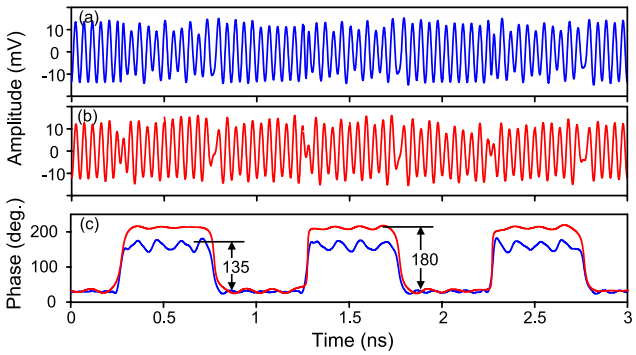

Fig. 3. Waveforms of the 2 Gbit/s, 21.92 GHz phase-coded signal when the voltage of the coding signal is (a) 1.5 and (b) 2 V, (c) the extracted phase shifts from (a) and (b).

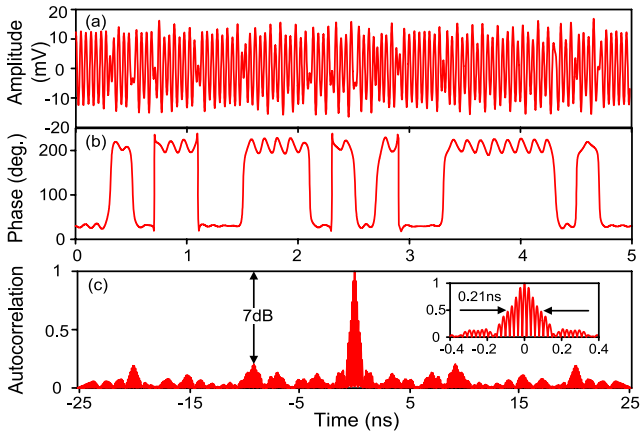

Fig. 4. (a) Waveform of the 5 Gbit/s, 21.92 GHz phase-coded signal, (b) the extracted phase shift, and (c) the autocorrelation. Inset: zoom-in on the peak of the autocorrelation.

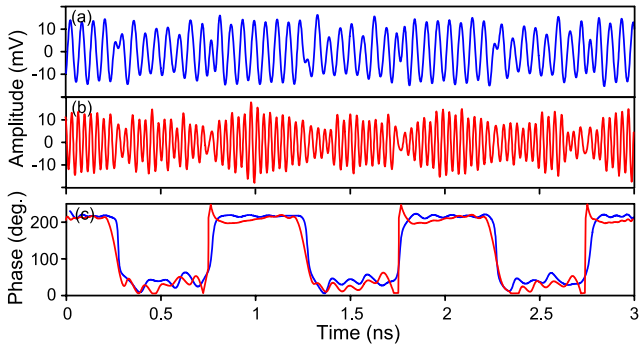

Fig. 5. Waveforms of the 2 Gbit/s phase-coded signal with frequency of (a) 16.48 and (b) 29.76 GHz, (c) the extracted phase shifts from (a) and (b).

signal can be extended up to the W-band considering that the bandwidth of the integrated modulator is 23 GHz. However, in the experiment, a higher frequency cannot be observed due to the limitation of the sampling rate of the oscilloscope (80 GS/s).

In the experiment, the drifting of the DC bias points in the modulator and the variation of the FBG may lead to poor stability. This problem can be resolved by employing a DP-QPSK modulator bias controller (i.e. YY LABS Inc. D0158) in the system and packaging the Sagnac loop.

In conclusion, we propose and demonstrate a photonic approach to generate a frequency-octupled phase-coded signal. The key component of the scheme is an integrated DP-QPSK modulator, which is employed to achieve the carrier-suppressed high-order double sideband modulation. Two fourth-order optical sidebands are generated through the modulator and then sent to an FBG-incorporated Sagnac loop to perform phase coding. The proposed scheme has large carrier frequency tunability, which can range from several MHz to beyond the W-band. The 2 Gbit/s phase-coded signals with frequencies at 16.48, 21.92, and 29.76 GHz are experimentally generated. The proposed approach can find applications in high frequency and frequency-agile radar systems and wireless communication systems.

This work was supported in part by the National Science Foundation of China (Nos. 61571461, 61401502, 61422108, and 61527820) and the Fundamental Research Funds for the Central Universities.

References

1. J. Lin, C. Lu, H. Chuang, F. Kuo, J. Shi, C. Huang, and C. Pan, IEEE Photon. Technol. Lett. **24**, 1437 (2012).
2. X. Li, J. Yu, J. Zhang, F. Li, Y. Xu, Z. Zhang, and J. Xiao, IEEE Photon. Technol. Lett. **26**, 1825 (2014).
3. C. Gao, S. Huang, J. Xiao, X. Gao, Q. Wang, Y. Wei, W. Zhai, W. Xu, and W. Gu, Chin. Opt. Lett. **13**, 010604 (2015).
4. J. Li, T. Ning, L. Pei, J. Zheng, J. Sun, Y. Li, and J. Yuan, Chin. Opt. Lett. **13**, 080606 (2015).
5. Y. Dong, Z. Liu, X. Wang, N. Deng, W. Xie, and W. Hu, Chin. Opt. Lett. **14**, 120006 (2016).
6. Y. Cheng, F. Hu, F. He, L Wu, and X. He, Chin. Opt. Lett. **14**, 062802 (2016).
7. J. Chou, Y. Han, and B. Jalali, IEEE Photon. Technol. Lett. **15**, 581 (2003).
8. C. Wang and J. P. Yao, IEEE Photon. Technol. Lett. **24**, 1493 (2012).
9. W. Li, W. Wang, W. Sun, L. Wang, and N. Zhu, Opt. Express **22**, 7446 (2014).
10. F. Zhang, X. Ge, B. Gao, and S. Pan, Opt. Express **23**, 21867 (2015).
11. L. Wang, W. Li, H. Wang, J. Zheng, J. Liu, and N. Zhu, IEEE Photon. Technol. Lett. **25**, 678 (2013).
12. H. Jiang, L. Yan, J. Ye, W. Pan, B. Luo, and X. Zou, Opt. Lett. **38**, 1361 (2013).
13. S. Liu, D. Zhu, Z. Wei, and S. Pan, Opt. Lett. **39**, 3958 (2014).
14. Z. Li, W. Li, H. Chi, X. Zhang, and J. Yao, IEEE Photon. Technol. Lett. **23**, 712 (2011).
15. Z. Li, M. Li, H. Chi, X. M. Zhang, and J. P. Yao, IEEE Microwave Wireless Compon. Lett. **21**, 694 (2011).
16. J. Xiao, Z. Zhang, X. Li, Y. Xu, L. Chen, and J. Yu, IEEE Photon. J. **7**, 7101206 (2015).
17. J. Xiao, X. Li, Y. Xu, Z. Zhang, L. Chen, and J. Yu, Opt. Express **23**, 24029 (2015).
18. X. Li, S. Zhao, Y. Zhang, Z. Zhu, and S. Pan, IEEE Photon. Technol. Lett. **28**, 1980 (2016).
19. Y. Painchaud, M. Aubé, G. Brochu, and M.-J. Picard, in *Bragg Gratings, Photosensitivity, and Poling in Glass Waveguides* (2010), paper BTuC3.